

# Reflection of resonant light from a plane surface of an ensemble of motionless point scatters: Quantum microscopic approach

A. S. Kuraptsev<sup>1</sup> and I. M. Sokolov<sup>1,2</sup><sup>1</sup>*Peter the Great St. Petersburg Polytechnic University, 195251, St. Petersburg, Russia*<sup>2</sup>*Institute of Analytical Instrumentation, Russian Academy of Sciences, 198103, St. Petersburg, Russia*

(Received 17 January 2015; published 13 May 2015)

On the basis of general theoretical results developed previously in [JETP **112**, 246 (2011)], we analyze the reflection of quaresonant light from a plane surface of dense and disordered ensemble of motionless point scatters. Angle distribution of the scattered light is calculated both for  $s$  and  $p$  polarizations of the probe radiation. The ratio between coherent and incoherent (diffuse) components of scattered light is calculated. We analyze the contributions of scatters located at different distances from the surface and determine on this background the thickness of surface layer responsible for reflected beam generation. The inhomogeneity of dipole-dipole interaction near the surface is discussed. We study also dependence of total reflected light power on the incidence angle and compare the results of the microscopic approach with predictions of the Fresnel reflection theory. The calculations are performed for different densities of scatters and different frequencies of a probe radiation.

DOI: [10.1103/PhysRevA.91.053822](https://doi.org/10.1103/PhysRevA.91.053822)

PACS number(s): 42.25.Dd, 42.50.Nn, 72.15.Rn

## I. INTRODUCTION

The vast majority of experimental optical detection methods are based on analysis of radiation scattered from the investigated medium. Among these methods ones based on measurements of a coherent component of scattered radiation have a range of advantages. Reflection of light from resonant media has even formed a special area of optics (see [1–16], and references therein). Among a great variety of resonant media the disordered ensembles of pointlike scatters in which motion can be neglected take a special place. The physical model of motionless scatterers is commonly used for a description of the interaction between impurity centers in solids and electromagnetic radiation. It also can be used for a description of cold atomic ensembles prepared in a special atomic trap.

Dense ensembles, in which the average interatomic distance and the mean free path of the photon are comparable with the wave length of resonant radiation, have attracted a special interest recently. It is connected with both exciting physical properties of such systems as its widespread practical application in quantum metrology, frequency standardization, and quantum information science [17–25].

The interaction of resonant light with dense ensemble has a range of important features which are usually neglected in the case of dilute ensembles. If the average interatomic distance is comparable with resonant wavelength the atoms cannot be considered as independent scatters of electromagnetic waves (hereafter we will associate point scatters with atoms for brevity). In this case we deal with so-called cooperative scattering [26,27]. Interatomic dipole-dipole interaction significantly influences the optical characteristics of a medium. Collective effects cause density-dependent shifts of atomic transition as well as distortion of spectral line shape [28,29]. The real part of dielectric permittivity of dense atomic ensemble can be negative in some spectral area [30,31].

Modification of optical characteristics caused by dipole-dipole interaction manifests itself differently for spatial areas inside the medium and near its surface. The atoms located in the subsurface layer interact predominantly with atoms situated at one side of them, inside the ensemble. The surface

layer is generated. Its width depends on density of the sample and is about 1.5–2 inverse wave numbers [32]. This subsurface region significantly influences both the incoherent scattering and coherent reflection.

The goal of this paper is to study the reflection of quaresonant light from the plane boundary between vacuum and dense ensemble of point scatters. We analyze the influences of the features of dipole-dipole interaction caused by the subsurface spatial inhomogeneity on the properties of reflection.

Inhomogeneity of the optical properties and spatial disorder of atoms in the ensemble restrict the classical description using Fresnel equations which require the mean free path of photon and the wavelength of probe radiation much greater than the average interatomic distance. In this paper we use the consequent quantum microscopic approach [26]. This approach allows us to obtain both coherent and incoherent (diffuse) components of scattered light. Note that nearly all previous applications of the method developed in [26] were devoted to analysis of incoherent scattering of the light from random media, particularly for study of multiple recurrent scattering. This analysis requires calculation of the average intensity of scattered light. In the present paper for the first time we use this approach for description of coherent mirror scattering from random media. We calculate the mean electric field of the light scattered by disordered media with a sharp boundary as a sum of individual contributions of all atoms. Such an approach allows us to analyze the partial contributions of the layers of the medium located at different distances from the surface and analyze the properties of reflected wave depending on density of the atoms, frequency of the probe light, its polarization, and on angle of incidence.

## II. BASIC ASSUMPTIONS AND APPROACH

The calculation of resonant reflection in this paper will be made on the basis of a microscopic quantum approach developed in [26]. This approach is based on the nonstationary Schrödinger equation for the wave function of the joint system consisting of  $N$  motionless atoms and electromagnetic field.

All atoms are assumed to be identical and have a ground state  $J = 0$  separated by the frequency  $\omega_0$  from an excited  $J = 1$  state. The excited state has the Zeeman structure so there are three sublevels for each atom which differ by the value of angular momentum projection  $m = -1, 0, 1$ . Such a structure of atomic levels allows us to describe the effects connected with the vector nature of the electromagnetic field in the case of the dense medium correctly. Note that the standard two-level scalar model does not have this advantage. For a detailed comparison of these models, see [33,34]. The Hamiltonian of the joined system  $H$  can be presented as a sum of two operators  $H_0 + V$ . Here  $H_0$  is the sum of the Hamiltonians of the free atoms and the free field, and  $V$  is the operator of their interaction. The wave function is found as an expansion in a set of eigenstates  $\{|l\rangle\}$  of the operator  $H_0$ .

The key simplification of the approach is in the restriction of the total number of states  $|l\rangle$  taken into account. We consider only the vacuum state  $\psi_{g'}$  (all atoms are in the ground state and there is no photon), the onefold excited atomic states  $\psi_{e_a^m}$  (one atom is excited and there is no photon), the onefold excited states of the field subsystem  $\psi_g$  (there is one photon and there are no excited atoms), and the nonresonant states  $\psi_{e_a^m e_b^{m'}}$  with two excited atoms and one photon in the field subsystem. The complex index  $e_a^m$  used here contains information about both the number of excited atom  $a$  and the Zeeman sublevel which is populated.

In the rotating wave approximation it is enough to take into account only the states  $\psi_{e_a^m}$  and  $\psi_g$ . States without excitation both in atomic and field subsystem  $\psi_{g'}$  allow us to describe coherent states of the weak probe radiation [35]. Nonresonant states with two excited atoms and one photon  $\psi_{e_a^m e_b^{m'}}$  are necessary for a correct description of the dipole-dipole interaction at short interatomic distances.

The amplitude of state  $\psi_{g'}$  does not change during the evolution of the system, because transitions to this state from other states taken into account are impossible. The transition from  $\psi_{g'}$  to any other state is also impossible. The total set of equations for the other quantum amplitudes  $b_{e_a^m}$ ,  $b_g$ , and  $b_{e_a^m e_b^{m'}}$  is infinite because of the infinite number of field modes. From this infinite set of equations we can pick out the finite subset of  $3N$  algebraic equations for the Fourier component of amplitudes of onefold atomic excitation  $b_{e_a^m}$ . Its formal solution can be written as follows:

$$b_{e_a^m}(\omega) = \sum_{b,m'} R_{e_a^m e_b^{m'}}(\omega) b_{e_b^{m'}}^0(\omega). \quad (2.1)$$

The matrix  $R_{e_a^m e_b^{m'}}$  is the resolvent of the considered system projected on the onefold atomic excited states. This matrix describes the multiple photon exchange among atoms and it depends both on the spatial location of atoms and on the frequency of probe light (see [26,31]). The vector  $b_{e_b^{m'}}^0(\omega)$  describes the interaction of atoms with external radiation which is assumed to be a plane monochromatic wave. This vector depends on the direction of probe light and its polarization.

$$b_{e_b^{m'}}^0(\omega) = -\mathbf{d}_{e_b^{m'};g_b} \mathbf{e} / \hbar E_0 \exp(i\mathbf{k}_0 \mathbf{r}_b). \quad (2.2)$$

In this equation  $\mathbf{d}_{e_b^{m'};g_b}$  is the dipole matrix element for transition from the ground  $g$  to the excited  $m'$  state of atom  $b$ ,

$E_0$  is an amplitude of probe radiation,  $\mathbf{k}_0$  and  $\mathbf{e}$  are its wave vector and unit polarization vector,  $\mathbf{r}_b$  is the radius vector of the atom  $b$ .

The microscopic approach allows us to consider an atomic ensemble with arbitrary shape and spatial distribution of atomic density. In this paper we will consider a sample in the form of a rectangular parallelepiped with random but uniform on average spatial distribution of atoms. The edge lengths of the parallelepiped are  $l_x$ ,  $l_y$ , and  $l_z$ . The quantization axis  $z$  is directed perpendicular to the front surface of an ensemble, the axis  $x$  along the projection of the wave vector of the probe light on this surface. The angle between the direction of probe light propagation and the axis  $z$  is  $\theta_0$ . The polarization of light is assumed to be linear. We will analyze two types of linear polarization: parallel to the plane of incidence ( $p$  polarization) and perpendicular to this plane ( $s$  polarization). The polarization vectors corresponding to these polarizations  $\mathbf{e}_p$  and  $\mathbf{e}_s$  can be presented in the basis of unit cyclic vectors  $\mathbf{e}_{-1}$ ,  $\mathbf{e}_0$ , and  $\mathbf{e}_{+1}$  using standard relations [36]. The advantage of this basis is that the dipole moment projections are given by simple equations  $\mathbf{d}_{e_b^{-1};g_b} \mathbf{e}_{-1} = \mathbf{d}_{e_b^0;g_b} \mathbf{e}_0 = \mathbf{d}_{e_b^+;g_b} \mathbf{e}_{+1} = \sqrt{3\hbar c^3 \gamma_0 / 4\omega_0^3}$  ( $\gamma_0$  is the natural linewidth).

Describing the polarization properties of scattered light we will use the frame of reference connected with the direction of scattered light (with the  $z'$  axis along the wave vector). It is connected with typical arrangement of polarization measurement when polarization analyzers are oriented in accordance with the direction of detected radiation. So long as our paper is devoted mainly on the investigation of coherent scattering we will further restrict ourselves to the case when both incident and scattered waves have the same type of polarization ( $s$  or  $p$ ).

Numerical calculation of the amplitudes  $b_{e_a^m}(\omega)$  on the basis of (2.1) and (2.2) allows us to obtain amplitudes of other quantum states  $b_g$  and  $b_{e_a^m e_b^{m'}}$ . Thus we can obtain the wave function and any physical observable, particularly electric field strength of scattered light and light intensity (see [26] for detail). It gives us opportunity to compare the results obtained in the framework of the quantum microscopic approach with Fresnel equations.

The angular distribution of scattered light power contains a speckle component because of light interference from a big number of randomly distributed point scatters. In experiments the radiation averaged over an area of a photodetector and integrated over a definite time interval is measured. Therefore in our calculations we perform multiple averaging of results over random spatial configurations of atoms by the Monte Carlo method. To analyze the coherent component of scattered light we average the electric field strength and then we calculate intensity of this component. To calculate total light intensity we average light intensity itself. Note also that this averaging allows taking into account partly the residual thermal motion in cold atomic ensembles.

### III. RESULTS AND DISCUSSION

#### A. Angular distribution of scattered light

We start with analysis of angular distribution of light scattered by the optically dense plate. Figure 1 shows the

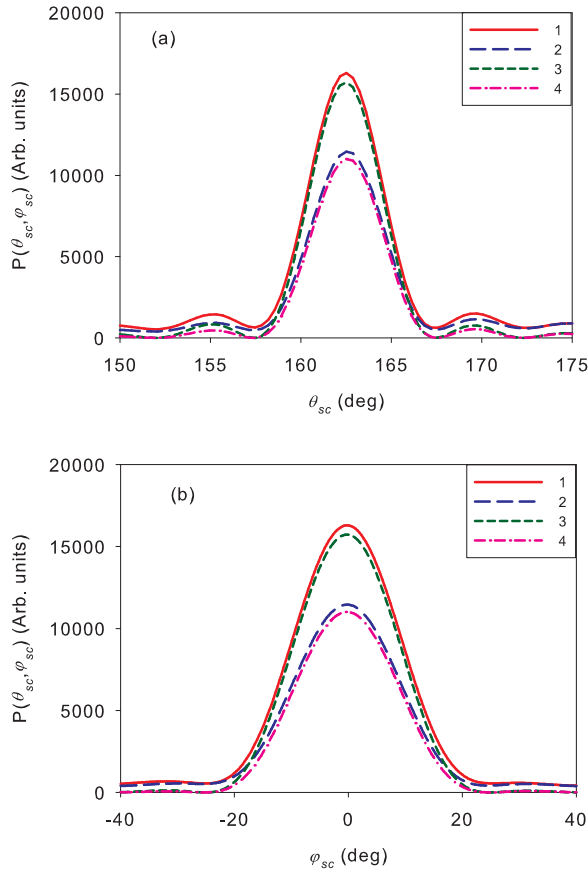


FIG. 1. (Color online) Angle distribution of the scattered light power. (a)  $\varphi_{sc} = 0$ , (b)  $\theta_{sc} = \pi - \theta_0$ . 1,  $s$  polarization; 2,  $p$  polarization; 3,  $s$ -coherent component; 4,  $p$ -coherent component.

power of light scattered in a unit spherical angle as a function of both the polar angle [Fig. 1(a)] and the azimuthal angle [Fig. 1(b)]. The calculation is performed for atomic ensemble with  $l_x = 110$ ,  $l_y = 55$ ,  $l_z = 6.53$  (hereafter in this paper we use the inverse wave number of resonant light  $k_0^{-1}$  as a unit of length,  $k_0^{-1} = \lambda_0/2\pi$ ). The probe radiation is assumed to be exactly resonant with free atom transition, its frequency detuning is equal to zero  $\Delta = \omega - \omega_0 = 0$ , and the angle of incidence is  $\theta_0 = 17.5^\circ$ . As the computational difficulty increases rapidly with the number of atoms the atomic density is chosen not very big  $n = 0.05$  which corresponds to the mean free path of photon  $l_{ph} = 1.63$ . However, as it was shown in [31] the collective effects caused by the dipole-dipole interaction play a significant role for such density.

Under considered conditions the reflection of light takes place not only from the front surface of the ensemble but from the side surfaces as well. To eliminate the influence of reflection from side surfaces we take into account only secondary radiation from atoms located sufficiently far from the sides, approximately 60% of the total number of atoms. In experiment such elimination can be performed by means of a diaphragm.

Figure 1(a) shows that the maximum of the scattered light power obtained in the frame of the microscopic approach corresponds to a well-known reflection law ( $\theta_{sc} = \pi - \theta_0$ ,  $\varphi_{sc} = 0$ ). Besides the main peak we observe weak satellite

peaks caused by diffraction from the rectangular front surface and a small contribution caused by diffuse scattering. The height and width of the main peaks in Figs. 1(a) and 1(b) are determined by the sizes  $l_x$  and  $l_y$ , respectively. As we have  $l_x > l_y$  the main peak of  $\theta$  distribution [Fig. 1(a)] is more narrow than the one of  $\varphi$  distribution [Fig. 1(b)].

For comparison we performed similar calculations for different sizes of atomic ensemble. The height of the main peak increased with size but its width decreased so that the total intensity of reflected light was proportional to the area  $l_x l_y$ .

In Fig. 1 we included the results of calculation of total scattered light power and its coherent component. The ratio of the coherent component to total power exceeds 0.85 even for relatively small atomic density  $n = 0.05$ . It confirms the fact that cooperative effects play a significant role for this density.

Note that there are several physically different cooperative effects which can take place under light interaction with dense and cold atomic ensembles. Such phenomena as superradiance, lasing in disordered media, and Anderson localization have attracted great attention recently. The physical effect studied in the present work has a bit different nature than all phenomena mentioned above. In our case collective effect does not assume multiple scattering. It is determined by interference of secondary radiation emitted by different atoms located in the subsurface layer of the cloud. Similar interference causes coherent Rayleigh forward scattering in which the cross section is proportional to the squared number of atoms in the ensemble. In our case intensity of reflected light is proportional to the squared amplitude of electric field and consequently to the squared number of atoms in the mentioned subsurface layer. In the next subsection we will analyze formation of the reflected beam in more detail.

## B. Microscopic analysis of reflected beam generation

Let us analyze now how the atoms located at different distances from the surface influence the reflected signal generation. Our approach allows us to calculate the reflected signal taking into account only the finite size layer near the front surface. Figure 2(a) shows corresponding results for three layers with the depth  $d = 0.5l_{ph}, l_{ph}, 2l_{ph}$  ( $l_{ph}$  is the mean free path of the photon obtained in [37]) as well as for the whole ensemble with depth  $7l_{ph}$ . In the case of the first and the second layers the power of reflected light exceeds the total reflected signal. For the third layer the result is less than one for a whole ensemble. Such behavior can be explained by the interference of the electromagnetic waves scattered by different atoms. When we consider relatively thin layers the phase increment on its thickness is small so the interference is constructive and the power of the reflected signal increases with the depth of layer. If thickness of the layer becomes comparable with wavelength the dephasing of electromagnetic waves scattered by different atoms becomes important and the destructive influence of the interference has to be taken into account. It looks like an interference of light in transparent thin films. But in our case we deal with resonant atomic ensembles and the absorption is very important. Under considered conditions the mean free path of the photon is approximately equal to a quarter of the resonant light wavelength. Atoms located sufficiently far

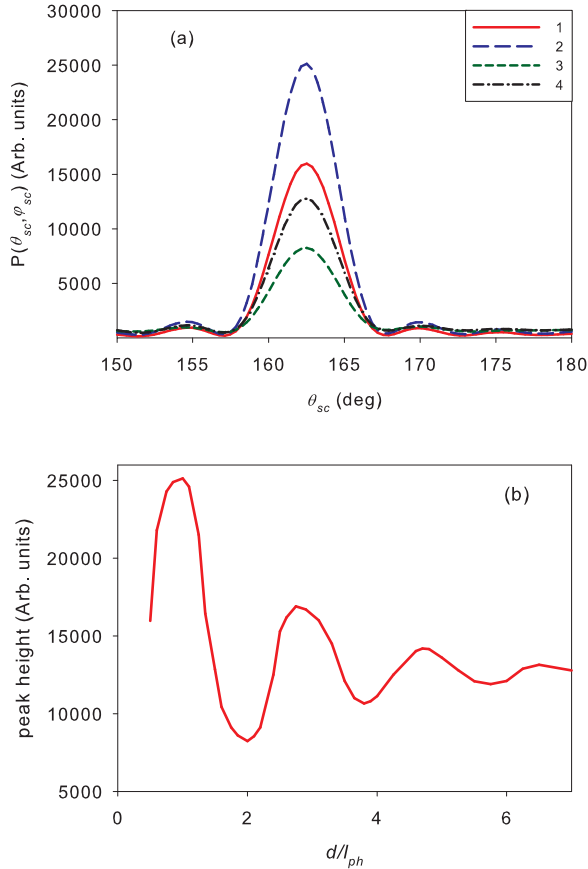


FIG. 2. (Color online) (a) Angle distribution of light scattered by subsurface layers.  $s$  polarization,  $\varphi_{sc} = 0$ ; depth of the layer: 1,  $0.5l_{ph}$ ; 2,  $l_{ph}$ ; 3,  $2l_{ph}$ ; 4,  $7l_{ph}$ . (b) Maximum of the function  $P(\theta_{sc}, \varphi_{sc})$  depending on the depth of the layer near the front surface;  $s$  polarization. For both figures  $n = 0.05$ ,  $\Delta = 0$ ,  $\theta_0 = 17.5^\circ$ ,  $l_x = 102$ ,  $l_y = 51$ ,  $l_z = 11.42$ .

from the front surface do not influence the coherent scattering, i.e., the reflection. This can be seen in Fig. 2(b). We observe saturation in the dependence of reflected light power on the depth of layer. The curve in Fig. 2(b) flattens out at depth of the layers greater than  $(3.5-4)l_{ph}$ . For bigger density the mean free path of the photon is smaller and the saturation is observed for smaller depth.

Note, however, that attenuation of the curve shown in the Fig. 2(b) is essentially slower than can be expected if we suggest wave damping taking into account its propagation in two directions—toward scattered atoms and from them outside the medium. Figure 2(b) shows the total contribution of atoms located inside the layer with thickness  $d$ . From this contribution we can calculate the partial contribution of atoms located in a thin layer situated at the arbitrary depth  $l$ . Corresponding analysis shows that this partial contribution decreases approximately exponentially  $\exp(-\alpha l / \cos \theta_0)$  (the deviation from exponential dependence connects with the boundary effects mentioned above). The index of exponential attenuation  $\alpha$  is close to the inverse mean free path of the photon in the considered medium  $\alpha \approx 1/l_{ph}$ . So this index is two times smaller as compared with its expected value if we consider light propagation in two directions. This discrepancy

connects with the fact that inside the atomic ensemble there is no coherent wave propagating in the “backward” direction (of course, if the medium is semi-infinite or if scattering from the far edge can be neglected). The reflected coherent light beam exists only outside the atomic ensemble and this beam is a result of collective scattering by all atoms of the ensemble. Figure 2 demonstrates that the determinative contribution to the reflection signal is given by the subsurface layer with the depth comparable with wavelength.

### C. Comparison with Fresnel equations

In this subsection we consider the dependence of the reflection coefficient on the angle of incidence and show that under considered conditions such dependence cannot be described by Fresnel equations.

Comparing our results with Fresnel theory we have to take into account that the angular size of the reflected light cone in our case is finite even for the plane incident wave because of the finite sizes of the front surface of the atomic sample. For this reason it is natural to determine the reflectivity  $R$  as the ratio of the light power in the main maximum of angular distribution  $P$  (see Fig. 1) to the total power of light scattered in all directions  $P_0$ .

$P$  can be obtained as an integral of the angular distribution of scattered light  $P(\theta_{sc}, \varphi_{sc})$  over the reflected light cone  $\Omega_c$ ,

$$P = \int_{\Omega_c} P(\theta_{sc}, \varphi_{sc}) d\Omega. \quad (3.1)$$

$P_0$  can be obtained using the optical theorem.

Figure 3 shows the dependence of reflectivity on the angle of incidence. Two couples of curves are shown. The first one is calculated on the basis of the microscopic approach and the second couple of curves is obtained from Fresnel equations. Dielectric permittivity required for the corresponding calculation was calculated by the method described in [30,37].

Figure 3 demonstrates that for the atomic density  $n = 0.05$  we have a good agreement between the quantum microscopic approach and Fresnel equations for  $p$  polarization. However for  $s$  polarizations there is noticeable quantitative disagreement

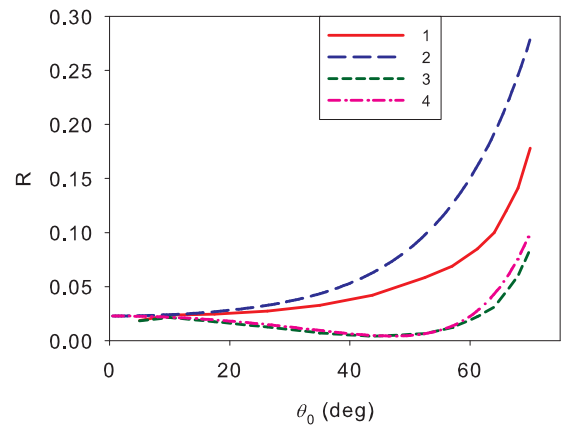


FIG. 3. (Color online) Dependence of reflectivity on the angle of incidence. 1 and 2,  $s$  polarization; 3 and 4,  $p$  polarization; 1 and 3, microscopic approach; 2 and 4, Fresnel equations. The parameters of the ensemble are the same as in Fig. 1.

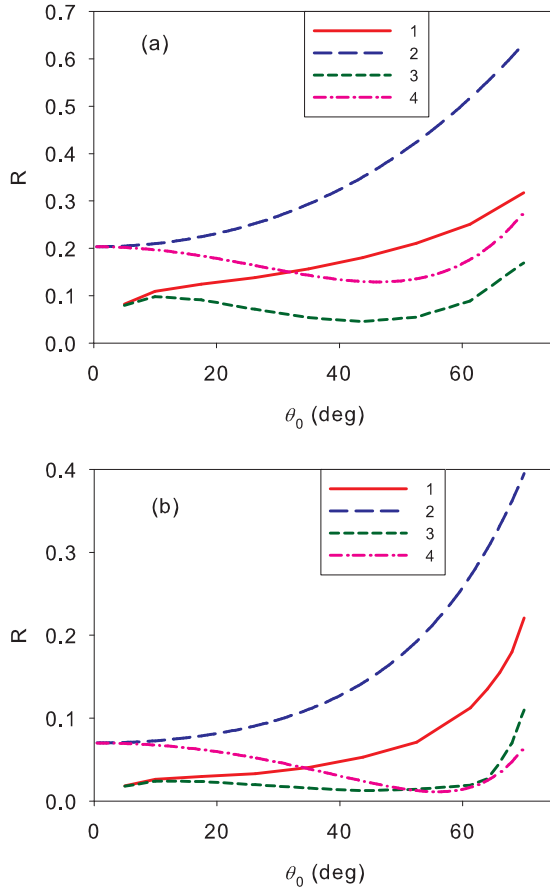


FIG. 4. (Color online) Reflection coefficient depending on the angle of incidence.  $n = 0.5$ ,  $\Delta = \gamma_0$  (a);  $\Delta = -\gamma_0$  (b); 1 and 2,  $s$  polarization; 3 and 4,  $p$  polarization; 1 and 3, microscopic approach; 2 and 4, Fresnel equations.

between these two approaches. The situation changes more dramatically for bigger densities.

Figure 4 shows the angular dependence of reflectivity for the atomic density  $n = 0.5$ . Resonant dipole-dipole interaction is so strong for this density that it causes a negative real part of the dielectric permittivity in some spectral area [30,31,37]. For example, for the probe light with detuning  $\Delta = \gamma_0$  the dielectric permittivity is equal to  $\varepsilon = -0.125 + 1.542i$ . The mean free path of the photon for these parameters is  $l_{ph} = 0.55$ . Curves in the Fig. 4(a) are calculated for this case. For comparison we add the plot corresponding to the negative detuning  $\Delta = -\gamma_0$  ( $\varepsilon = 1.80 + 1.40i$ ). The mean free path of the photon for this detuning is  $l_{ph} = 1.03$ . Note that the dielectric permittivity was calculated in [37] for spatially homogeneous (on average) atomic ensembles by the analysis of light propagation sufficiently far from their boundaries.

From Fig. 4 it is clearly seen that results obtained in the frame of the microscopic approach differs essentially from predictions of Fresnel equations for both polarization channels as well as for both considered detunings  $\Delta = \gamma_0$  and  $\Delta = -\gamma_0$ .

In our opinion there are two main reasons for such a discrepancy. First of all Fresnel equations require that averaged interatomic separations should be much less than

light wavelength and the photon mean free path in considered medium. In our case it is not so. Both the wavelength and mean free path of the photon are comparable with interatomic separations. The second important peculiarity of considered physical conditions is the essential role of boundary effects. As we showed in the previous subsection under resonant reflection the main contribution into the reflected signal is given by the surface layer in which depth is about several mean free paths of the photon. But just in this spatial domain the inhomogeneity in optical properties of a medium caused by the features of resonant dipole-dipole interaction is very essential [32]. Atoms located in the surface layer responsible for the reflected signal are in different physical condition as compared with atoms located inside the medium.

At the end of this section note that the important feature of the quantum microscopic approach used in this work is that the resolvent matrix (2.1) is determined numerically so it does not allow us to consider atomic ensemble with a very large number of atoms. The calculations described in this paper were made for 2000–7000 atoms. In this regard, to make sure that observed results are not caused by the small size of the cloud we repeated for comparison our calculations for different sizes of the front surface of the atomic ensemble. We increased the area of the front surface from 1.2 to 1.6 times and the difference in the reflection coefficient was at the level of computational error caused by statistical error of Monte Carlo averaging mainly.

#### IV. CONCLUSION

In this paper we analyze the reflection of quasiresonant light from a plane surface of dense and disordered ensemble of motionless point scatters like impurity centers in solid. The calculation is performed on the basis of the quantum microscopic approach. Solving the nonstationary Schrödinger equation for the joint system consisting of atoms and a weak electromagnetic field we calculate angular and polarization characteristics of light scattered by an ensemble in the form of a rectangular parallelepiped with big optical depth. The ratio between coherent and incoherent (diffuse) components of scattered light is also studied.

The microscopic approach allows us to analyze the influence of scatters located at different distances from the surface. This analysis shows that the main contribution into reflected light comes from the surface layer in which depth is determined by several mean free paths of the photon in the considered medium. It proves that the inhomogeneity of dipole-dipole interaction near the surface essentially influences the coherent reflection.

We studied the dependence of total reflected light power on the incidence angle for both  $s$  and  $p$  polarizations. The calculations are performed for different densities of scatters and different frequencies of a probe radiation. The reflection coefficient obtained in the framework of the quantum microscopic approach is compared with Fresnel equations. It is shown that a disagreement between two approaches increases with atomic density. This discrepancy is explained by subsurface violation in the spatial homogeneity of the medium and by the fact that for resonant light the mean free path of the photon is comparable with the average interatomic distance.

It is shown that an important parameter here is  $k_0 l_{ph}$ . A disagreement between two approaches increases with decrease of the value  $k_0 l_{ph}$ .

We expect that observed disagreement between the quantum microscopic approach and Fresnel equations (in the case of resonant light) will be especially important for the case of light reflection from thin films. If the thickness of the film is comparable with the resonant wavelength we can consider the whole volume of the medium as the subsurface area. The approach employed in the present work can be successfully used for this case even for films with inhomogeneous spatial distribution of atomic density. Furthermore, our approach allows one to describe the light scattering by nanoclusters with a small number of atoms.

In our opinion, microscopic analysis of resonant reflection performed here will be useful for further improvement of optical detection methods based on coherent scattering of resonant light.

#### ACKNOWLEDGMENTS

We acknowledge financial support from the Russian Foundation for Basic Research (Grant No. RFBR-15-02-01013) and from the Ministry of Education and Science of the Russian Federation (State Assignment 3.1446.2014K). A.S.K. also appreciates financial support from the RFBR (Grant No.14-02-31422), the Council for Grants of the President of the Russian Federation, and the nonprofit foundation “Dynasty.”

- 
- [1] E. V. Timoshchenko, V. A. Yurevich, and Yu. V. Yurevich, *Tech. Phys.* **58**, 251 (2013).
- [2] A. E. Kaplan and S. N. Volkov, *Phys. Rev. Lett.* **101**, 133902 (2008).
- [3] S. N. Volkov and A. E. Kaplan, *Phys. Rev. A* **81**, 043801 (2010).
- [4] A. V. Sel'kin, Yu. N. Lazareva, and V. A. Kosobukin, *J. Opt. Technol.* **78**, 519 (2011).
- [5] V. A. Sautenkov, H. Li, M. A. Gubin, Yu. V. Rostovtsev, and M. O. Scully, *Laser Physics* **21**, 153 (2011).
- [6] L. Velichanskii, R. G. Gamidov, G. T. Pak, and V. A. Sautenkov, *JETP Lett.* **52**, 136 (1990).
- [7] Ya. A. Fofanov, *Quantum Electron.* **39**, 585 (2009).
- [8] I. V. Zlodeev, Yu. F. Nasedkina, and D. I. Sementsov, *Opt. Spectrosc.* **113**, 208 (2012).
- [9] Yu. F. Nasedkina and D. I. Sementsov, *Opt. Spectrosc.* **104**, 591 (2008).
- [10] G. Nienhuis, F. Schuller, and M. Ducloy, *Phys. Rev. A* **38**, 5197 (1988).
- [11] M. G. Benedict and E. D. Trifonov, *Phys. Rev. A* **38**, 2854 (1988).
- [12] Ya. A. Fofanov and A. A. Rodichkina, *Opt. Spectrosc.* **103**, 322 (2007).
- [13] G. Nienhuis and F. Schuller, *Phys. Rev. A* **50**, 1586 (1994).
- [14] J. Guo, J. Cooper, A. Gallagher, and M. Lewenstein, *Opt. Commun.* **110**, 732 (1994).
- [15] H. Li, T. S. Varzhapetyan, V. A. Sautenkov, Y. V. Rostovtsev, H. Chen, D. Sarkisyan, and M. O. Scully, *Appl. Phys. B* **91**, 229 (2008).
- [16] H. Li, V. A. Sautenkov, Y. V. Rostovtsev, and M. O. Scully, *J. Phys. B: At. Mol. Opt. Phys.* **42**, 065203 (2009).
- [17] C. Cohen-Tannoudji, Nobel Prize in Physics Lecture (College de France et Laboratoire Kastler Brossel\* de l'Ecole Normale, Paris, 1997).
- [18] E. Bimbard, R. Boddada, N. Vitrant, A. Grankin, V. Parigi, J. Stanojevic, A. Ourjoutsev, and P. Grangier, *Phys. Rev. Lett.* **112**, 033601 (2014).
- [19] D. Loss and D. P. DiVincenzo, *Phys. Rev. A* **57**, 120 (1998).
- [20] K. A. Barantsev and A. N. Litvinov, *J. Exp. Theor. Phys.* **118**, 569 (2014).
- [21] G. Wilpers, T. Binnewies, C. Degenhardt, U. Sterr, J. Helmcke, and F. Riehle, *Phys. Rev. Lett.* **89**, 230801 (2002).
- [22] I. Courtillot, A. Quessada, R. P. Kovacich, A. Brusch, D. Kolker, J.-J. Zondy, G. D. Rovera, and P. Lemonde, *Phys. Rev. A* **68**, 030501(R) (2003).
- [23] F. X. Esnault, N. Rossetto, D. Holleville, J. Delporte, and N. Dimarcq, *Adv. Space Res.* **47**, 854 (2011).
- [24] D. Bouwmeester, A. Ekert, and A. Zeilinger, *The Physics of Quantum Information* (Springer-Verlag, Berlin, 2001).
- [25] J. S. Hodges, L. Li, M. Lu, E. H. Chen, M. E. Trusheim, S. Allegri, X. Yao, O. Gaathon, H. Bakhru, and D. Englund, *New J. Phys.* **14**, 093004 (2012).
- [26] I. M. Sokolov, D. V. Kupriyanov, and M. D. Havey, *J. Exp. Theor. Phys.* **112**, 246 (2011).
- [27] I. M. Sokolov, A. S. Kuraptsev, D. V. Kupriyanov, M. D. Havey, and S. Balik, *J. Mod. Opt.* **60**, 50 (2013).
- [28] T. Ido, T. H. Loftus, M. M. Boyd, A. D. Ludlow, K. W. Holman, and J. Ye, *Phys. Rev. Lett.* **94**, 153001 (2005).
- [29] A. S. Kuraptsev and I. M. Sokolov, *Phys. Rev. A* **90**, 012511 (2014).
- [30] Ya. A. Fofanov, A. S. Kuraptsev, and I. M. Sokolov, *Opt. Spectrosc.* **112**, 401 (2012).
- [31] I. M. Sokolov, M. D. Kupriyanova, D. V. Kupriyanov, and M. D. Havey, *Phys. Rev. A* **79**, 053405 (2009).
- [32] Ya. A. Fofanov, A. S. Kuraptsev, I. M. Sokolov, and M. D. Havey, *Phys. Rev. A* **87**, 063839 (2013).
- [33] I. M. Sokolov, D. V. Kupriyanov, R. G. Olave, and M. D. Havey, *J. Mod. Opt.* **57**, 1833 (2010).
- [34] S. E. Skipetrov and I. M. Sokolov, *Phys. Rev. Lett.* **112**, 023905 (2014).
- [35] L. Mandel and E. Wolf, *Optical Coherence and Quantum Optics* (Cambridge University Press, Cambridge, 1995).
- [36] D. A. Varshalovich, A. N. Moskalev, and V. K. Khersonskiy, *Quantum Theory of Angular Momentum* (World Scientific, Singapore, 1988).
- [37] Ya. A. Fofanov, A. S. Kuraptsev, I. M. Sokolov, and M. D. Havey, *Phys. Rev. A* **84**, 053811 (2011).